

DETERMINATION OF THE SURFACE TOPOGRAPHY IN RILL EROSION BY IMAGING TECHNIQUES

Kürşad ERDOĞAN¹ and Fikret ARI¹


¹Department of Electrical and Electronics Engineering,
Ankara University, Ankara, TURKEY

ABSTRACT. Soil erosion, mainly occurring in agricultural areas, is an economic and ecological problem that can happen anywhere. Swelling and transport of soil particles reduce the productivity of agricultural lands. Soil surface analysis and soil-water interaction are essential topics in agricultural research and engineering as they affect the risk of soil erosion. Erosion affects the upper soil layers rich in organic matter. After the transport of this topsoil, the subsoil with a more compact structure emerges. In this case, the cultivation of the soil becomes complex, and agricultural productivity is adversely affected. Different techniques have been used to analyze the effects of erosion. In this study, we focused on rill erosion, one of the types. An electronic imaging system has been designed using the Microsoft Kinect Sensor and Raspberry Pi, which can be found quickly and at a low cost during operation. The software has been developed to extract the surface topography by analyzing the depth images of rill erosion obtained with this system. Measurements were taken using eight types of flow rates on four soil types. As a result of the experimental findings, it has been seen that volume changes of 1.3812 mm³ can be detected as a unit with the Kinect Sensor placed at a distance of 70 cm.

1. INTRODUCTION

Erosion is the carrying and sweeping of the soil by flood waters and winds from other external forces, especially rivers. Soil erosion, especially in agricultural areas, is an economic and ecological problem that can occur anywhere. Swelling and transport of soil particles reduce farmland productivity [1]. Soil surface analysis and soil-water interaction are essential topics in agricultural research and engineering as they affect the risk of soil erosion [2]. Erosion affects the upper soil layers rich in

Keywords. Rill erosion, depth image, kinect sensor, raspberry pi, mobile systems, surface topography.

✉ erdogank@ankara.edu.tr -Corresponding author;  0000-0001-5178-0930

✉ fari@eng.ankata.edu.tr;  0000-0002-6104-4467.

organic matter. After the transport of this topsoil, the subsoil with a more compact structure emerges. In this case, soil cultivation becomes difficult, and agricultural productivity is adversely affected.

One of the forms of soil erosion, mainly caused by precipitation or water accumulation, is rill erosion. It is a type of erosion that occurs in the form of small channels formed by the collection of stream water, initiating a flow from weak and loose areas in the soil and dragging the soil during this flow [3]. When examining the damages caused by soil erosion, it is imperative to analyze the topography, which is the shape of the details of the land surface.

Many techniques have been developed for topography analysis. Terrestrial Laser Scanners [4], LiDAR (Light Detection and Ranging) [2], Unmanned Aerial Vehicles [3], and Digital cameras [5] were used to extract the topography.

It is considered that Microsoft Kinect-style depth sensing units and portable mini computer systems such as Raspberry Pi can be used in soil erosion analysis due to their low cost and ease of use. It is thought that the obtained topography results will positively contribute to protecting agricultural lands and increasing their productivity.

Raspberry Pi has been used in this study because of its flexible programming, small size, cheapness, and ease of supply. With the Python software developed on Raspberry Pi, depth images, including distance information, were obtained via Kinect Sensor. The topographies of rill-eroded areas on these images were extracted using image processing algorithms with MATLAB software. The extracted topography was analyzed, and evaluations were made on the soil losses after erosion.

A cheaper and more practical solution has been developed using mobile technologies to obtain a depth image using the Raspberry Pi and Kinect Sensor. Depth images can be obtained remotely by connecting to Raspberry Pi with mobile phones. Figure 1 shows the Python application running on a mobile phone with an Android operating system. Contribution of this paper, a simple and cost-effective system is proposed to analyze the effect of rill erosion.

2. MATERIAL AND METHODS

2.1. Structure of the Developed System. The system in Figure 2 is designed to extract the topography of rill erosion. Python libraries were installed on Raspberry Pi, and Python software was developed to take depth images via Kinect Sensor. Using the depth images obtained with developed software, the surface topography was obtained using image processing techniques with MATLAB software.

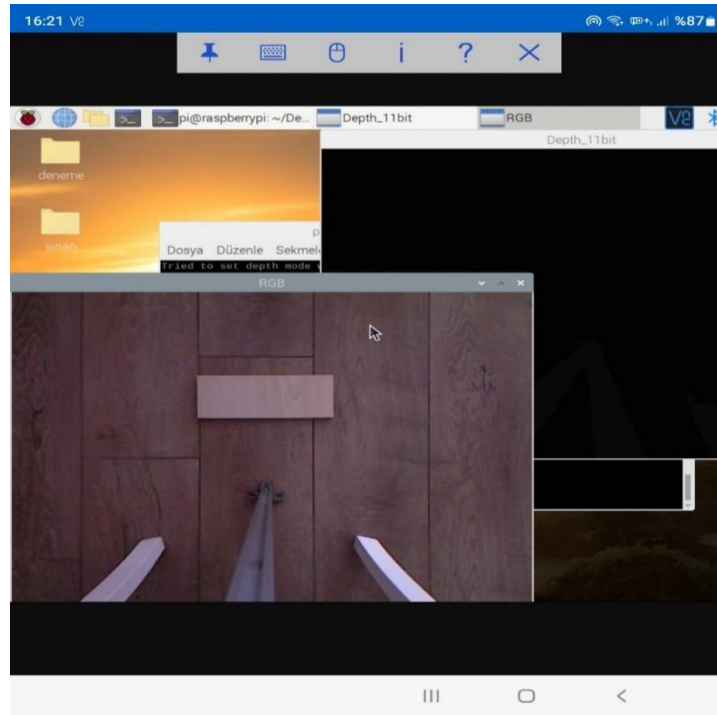


FIGURE 1. Depth and RGB image acquisition via Mobile Phone.

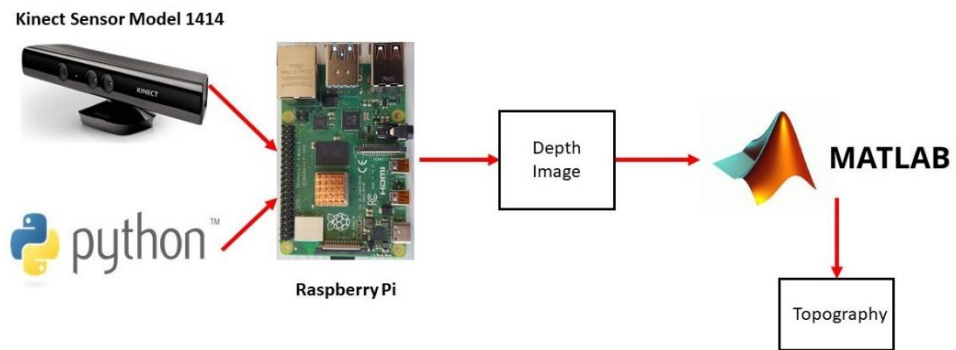


FIGURE 2. Designed system.

2.2. Experimental Measuring Setup. The mechanism was prepared in the Mechanical Production Laboratory and Electronics Development and Research Laboratory in the Department of Electrical and Electronics Engineering at Ankara University. This mechanism is the “Rill Erosion Measuring Device,” which can also be expressed as a V-shaped small groove measurement setup created to measure the properties of soils against rill erosion at different flow values in the laboratory environment [6]. The Kinect Sensor was placed at a height 70 cm from the Rill Erosion Measuring Mechanism, and its connection with the Raspberry Pi was ensured. Depth images were taken by connecting a computer or mobile phone with a Raspberry Pi via Wi-Fi access. The experimental setup created is shown in Figure 3.

Raspberry Pi is Linux-based hardware developed for simple computer science learning. It has started to be used widely because it can perform most functions that a computer can do, can be programmed for different purposes, and is small in size and affordable. Raspberry Pi 4 Model B was used in the experimental study.

Kinect Sensor is a product initially developed by Microsoft for motion detection for the Xbox game console. With the microphone, RGB camera, depth sensor, and cheap cost, this product has started to be used for many applications besides being an additional device for a game console. Studies have been carried out on its usability for many applications, thanks to its hardware that allows real-life applications to be developed [7]. Kinect Sensor's RGB camera produces 8-bit video with a resolution of 640x480 pixels. The IR camera can create an 11-bit depth image with a resolution of 640x480 pixels [8].

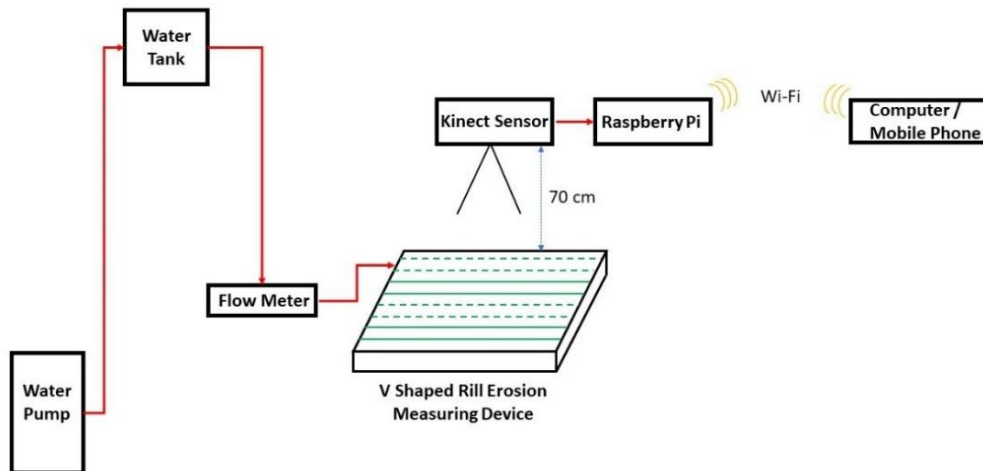


FIGURE 3. Experimental setup.

The raw values in the depth images obtained with the Kinect Sensor must be converted to values containing distance information in mm. For each pixel value, the distance value in mm is calculated by using the formulation in Equation 1 [9] with MATLAB program.

$$Distance = 1000 * \left[k1 * \tan \left(\frac{RawDepth}{k2} + k3 \right) \right] \quad (1)$$

The coefficients used in Equation 1 are $k1 = 0.1236$, $k2 = 2,842.5$, $k3 = 1.1863$.

Kinect Sensor makes IR radiation with the IR projector. The IR camera detects the reflection of this IR radiation from the environment. The Kinect Sensor creates depth images through the relationship between this radiation and reflection. Various noises may also occur in the depth images created by the Kinect Sensor. In the experimental studies, "Unmeasurable Depth" noises, where the depth value cannot be measured, may occur in the depth calculation of the objects located very close to or far from the Kinect Sensor. This may appear due to discontinuities on the surface, reflections, shadows, or other reasons [10].

To eliminate the immeasurable depth noise on the depth images containing the distance information obtained, it is necessary to search for this error in each pixel of the 640x480 pixel image and take action to correct the defective pixel. For this, a 5x5 filter was used on the image.



FIGURE 4. Test setup designed for the creation of the reference table.

After all these processes, it is necessary to calculate how much surface area each pixel in the surface topography corresponds to. The test setup in Figure 4 was prepared to create a reference table based on the distance of the Kinect Sensor to the relevant surface. Depth images were taken over the reference object by placing the Kinect Sensor at 1 cm distances between 70 cm and 80 cm. The area of the real object is divided by the area of the depth image in pixels. The reference table in Table 1 was created with the calculated values.

The actual volume of the object used in Figure 4 was calculated with the designed setup with a difference of 5.8 mm^3 (Table 2).

TABLE 1. Reference table.

Distance of Kinect Sensor to Object (cm)	Total Number of Pixels	Area Corresponding to 1 Pixel (mm^2)
70	13,698	1.3812
71	13,433	1.4085
72	12,894	1.4674
73	12,799	1.4782
74	12,283	1.5403
75	12,009	1.5755
76	11,697	1.6175
77	11,637	1.6259
78	11,027	1.7158
79	11,026	1.7159
80	10,681	1.7714

3. RESULTS AND DISCUSSION

Rill erosion was created by placing four types of soil, shown in Figure 5, into the V-shaped rill erosion measurement setup, and flowing water at a flow rate of 0.10, 0.20, 0.30, 0.40, 0.50, 0.60, 0.70, and 0.80 for 3 minutes for each.

TABLE 2. Test results.



	Reference		MATLAB Measurement
			
Vertical (mm)	86	Total Pixels	13,698
Horizontal (mm)	220	Unit Area (mm ²)	1.3812
Height (mm)	18	Height (mm)	18
Volume (mm ³)	340,560	Volume (mm ³)	340,554.20



FIGURE 5. Soil types used in experimental study.

Information on the regions from which soil samples were taken and used in the experimental study is given in Table 3.

Rill erosion was created at the flow as mentioned above rates for each soil type, respectively. The RGB image was taken with a digital camera (a mobile phone with an Android operating system). Depth images were taken with the Kinect Sensor. An example of the captured images is given in Figure 6.

TABLE 3. Information on the region where the soil sample was taken.

Type of Soil	City / Town	Coordinates		Land Use
		Y	X	
S1 (Clay Soil)	Ankara/Ayaş	36449767E	4444604N	Plowed land (garden)
S2 (Silty Clay Soil)	Ankara/Polatlı	36427979E	4351404N	Plowed wheat stubble
S3 (Silty Clay Soil)	Ankara/Polatlı	36429841E	4350492N	Plowed land (garden)
S4 (Clay Soil)	Ankara/Polatlı	36423323E	4353041N	Sugar beet field

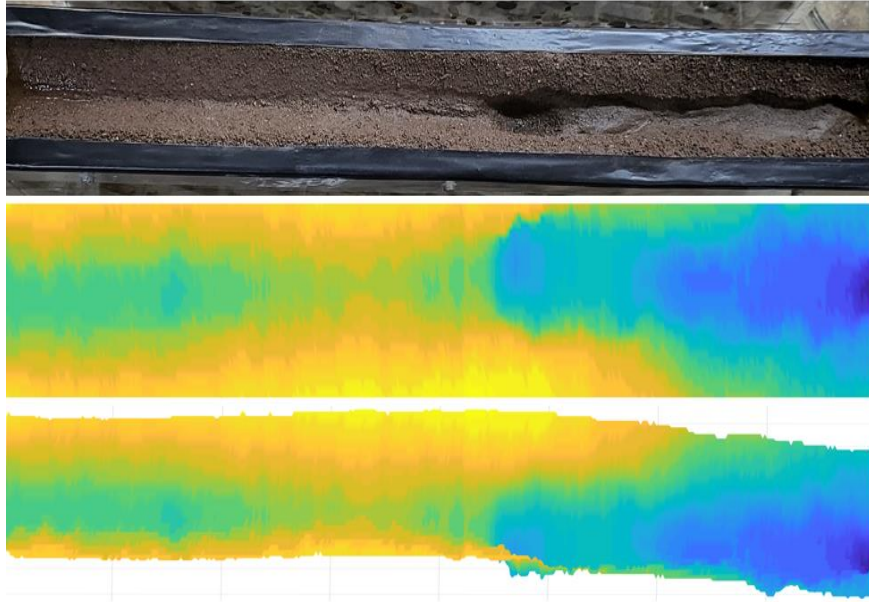


FIGURE 6. Soil 2, image after 0.80 flow.

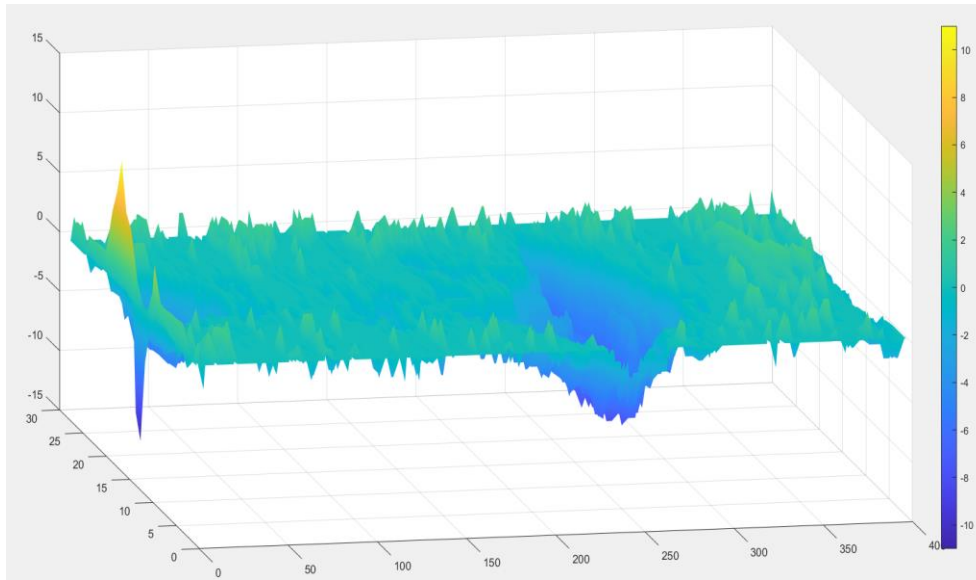


FIGURE 7. Soil 4, Comparison of soil movements between 0.10 – 0.80 flow rate.

To calculate the soil losses after the water flows on the soil samples, the surface topographies obtained as a result of both flows were subtracted from each other, and different images were obtained. The difference images of the depth images formed after 0.10 flow and 0.80 flow water flow were obtained to control the calculations. An example of the calculated difference images is given in Figure 7.

As seen in Figure 3, the Kinect Sensor is placed at the height of 70 cm. When calculating the lost soil volume, the difference between pixels with negative values and pixels with positive values is taken. The resulting difference in pixel value gives the height values in mm to be included in the volume calculation. The volume value of the lost soil was calculated by multiplying each pixel value (height) with the area value of 1.3812 mm^2 corresponding to 70 cm in the reference table in Table 1.

During erosion, soil loss occurs due to water flow. Depending on the characteristics of the soil type used, displacement of the soil without loss due to water entrainment and swelling of the soil with water may also occur. Negative values in Figure 7 indicate soil loss and positive values indicate soil areas that have been transported or swelled by water.

The volume calculations for the soil losses calculated depending on the soil types are shown in Tables 4 and 5 below.

When examining the difference between 0.20 and 0.30 flow rates for Soil 1, the

amount of soil loss due to erosion was less than soil movement or swelling. The amount of lost soil is calculated between flow rates; when the difference between the initial flow (0.10 flow) and the final flow (0.80 flow) is compared with the soil loss, it is seen that the difference is only 0.28 mm³.

The amount of lost soil calculated between flow rates for Soil 2. When the difference between the initial flow (0.10 flow) and the final flow (0.80 flow) is compared with the soil loss, it is seen that the difference is only 0.21 mm³.

The amount of lost soil is calculated between flow rates for Soil 3. When the difference between the initial flow (0.10 flow) and the final flow (0.80 flow) is compared with the soil loss, it is seen that the difference is only -0.01 mm³.

When examining the difference between 0.10 and 0.20 flow rates and 0.60 and 0.70 flow flows for Soil 4, the amount of soil loss due to erosion was less than soil movement or swelling. The amount of lost soil is calculated between flow rates; when the difference between the initial flow (0.10 flow rate) and the final flow (0.80 flow) is compared with the soil loss, it is seen that the difference is only -0.09 mm³.

TABLE 4. Rill erosion soil loss analysis (Soil 1 and 2).

Flows	Soil 1			Soil 2		
	Loss Soil (mm ³)	Carrying or Sweeping Soil (mm ³)	Total Loss Soil (mm ³)	Loss Soil (mm ³)	Carrying or Sweeping Soil (mm ³)	Total Lost Soil (mm ³)
0.10-0.20	3,436.40	1,041.40	2,395.00	4,606.30	2,558.00	2,048.30
0.20-0.30	2,250.00	5,588.30	-3,338.30	4,215.40	701.65	3,513.75
0.30-0.40	5,908.80	483.42	5,425.38	2,292.80	366.02	1,926.78
0.40-0.50	17,291.00	3,375.70	13,915.30	1,780.40	993.09	787.31
0.50-0.60	5,522.00	1,421.30	4,100.70	3,935.00	946.12	2,988.88
0.60-0.70	12,224.00	1,831.50	10,392.50	5,777.60	871.54	4,906.06
0.70-0.80	18,362.00	1,436.40	16,925.60	8,465.40	2,808.00	5,657.40
		Total	49,816.18		Total	21,828.48
0.10-0.80	51,146.00	1,330.10	49,815.90	22,715.00	886.73	21,828.27
		Difference	0.28		Difference	0.21

TABLE 5. Rill erosion soil loss analysis (Soil 3 and 4).

Flows	Soil 3			Soil 4		
	Loss Soil (mm ³)	Carrying or Sweeping Soil (mm ³)	Total Loss Soil (mm ³)	Loss Soil (mm ³)	Carrying or Sweeping Soil (mm ³)	Total Lost Soil (mm ³)
0.10-0.20	5,678.10	1,296.90	4,381.20	932.31	2,769.30	-1,836.99
0.20-0.30	4,320.40	2,466.80	1,853.60	3,366.00	1,379.80	1,986.20
0.30-0.40	6,348.00	2,248.60	4,099.40	4,838.30	1,256.90	3,581.40
0.40-0.50	7,794.10	2,839.70	4,954.40	4,917.10	1,975.10	2,942.00
0.50-0.60	7,165.70	2,006.90	5,158.80	2,977.90	1,370.20	1,607.70
0.60-0.70	5,180.90	1,426.80	3,754.10	2,298.30	2,342.50	-44.2
0.70-0.80	5,857.70	3,575.90	2,281.80	6,798.30	1,134.00	5,664.30
		Total	26,483.30		Total	13,900.41
0.10-0.80	27,388.00	904.69	26,483.31	15,301.00	1,400.50	13,900.50
		Difference	-0.01		Difference	-0.09

4. CONCLUSIONS

Rill erosion causes the fertile topsoil to drift by starting to flow from weak and loose areas in the soil due to precipitation or water accumulation. As a result, subsoil with a more compact structure emerges. In this study, a simple and cost-effective system is proposed to analyze the effects of rill erosion, frequently encountered in nature. System was realized with Kinect Sensor and Raspberry Pi in hardware and Python and MATLAB in software. Rill erosion effects of simulated various flow rates on soil types were analyzed. The soil volume lost due to rill erosion was calculated with the analyses made. By examining the depth images obtained, the displacement of the soil particles and the soil areas swelling with water were also visualized as soil loss. When the depth images obtained after the system created with the images obtained with the digital camera were examined, it was seen that the topography of rill erosion was revealed harmoniously. With the Kinect Sensor placed at the height of 70 cm,

volume changes of 1.3812 mm³ could be detected as a unit. It has been observed that the system developed independently of soil types gives consistent results. It is considered that the system will be portable and low-cost to provide ease of use in the field. In future studies, this system will be easily integrated into remote measurement systems to monitor areas that may be exposed to rill erosion continuously.

Author Contribution Statements The authors contributed equally to this work.

Declaration of Competing Interests The authors declare that they have no known competing financial interests or personal relationships that could have appeared to influence the work reported in this paper.

Acknowledgment The authors gratefully acknowledge Assoc. Prof. Dr. Selen Deviren Saygın, Soil Scientist from Ankara University Department of Soil Science and Plant Nutrition for her constructive and helpful comments and recommendations. This work was partially supported by the Scientific and Technological Research Council of Turkey [TÜBİTAK-3001, Project no: 118O111].

REFERENCES

- [1] Rieke-Zapp, D. H., Nearing, M. A., Digital close range photogrammetry for measurement of soil erosion, *Photogramm. Rec.*, 20 (109) (2005), 69-87.
- [2] Foldager, F. F., Pedersen, J. M., Skov, E. H., Evgrafova, A., Green, O., LiDAR-Based 3D scans of soil surfaces and furrows in two soil types, *Sensors*, 19 (3) (2019), 661, <https://doi.org/10.3390/s19030661>.
- [3] Stefano, C. D., Palmeri, V., Pampalone, V., An automatic approach for rill network extraction to measure rill erosion by terrestrial and low-cost unmanned aerial vehicle photogrammetry, *Hydrol. Process.*, 33 (2019), 1883-1895, <https://doi.org/10.1002/hyp.13444>.
- [4] Eitel, J. U. H., Williams, C. J., Vierling, L. A., Al-Hamdan, O. Z., Pierson, F. B., Suitability of terrestrial laser scanning for studying surface roughness effect on concentrated flow erosion processes in rangelands, *Catena*, 87 (3) (2011), 398-407, <https://doi.org/10.1016/j.catena.2011.07.009>.
- [5] Li, P., Ucgul, M., Lee, S. H., Saunders, C., A new method to analyse the soil movement during tillage operations using a novel digital image processing algorithm, *Comput. Electron. Agric.*, 156 (2019), 43-50, <https://doi.org/10.1016/j.compag.2018.11.009>.
- [6] Saygın, S. D., Süreç tabanlı modellemede parmak erozyonu toprak duyarlılığı parametresinin fiziksel olarak belirlenmesi, (2020). Program Kodu: 3001 Başlangıç AR-GE. Proje No: 1180111.
- [7] Sharma, K., Kinect sensor based object feature estimation in depth images, *IJSIP*, 8 (12)

- (2015), 237-246, <http://dx.doi.org/10.14257/ijcip.2015.8.12.23>.
- [8] Mobini, A., Behzadipour, S., Foumani, M. S., Accuracy of kinect's skeleton tracking for upper body rehabilitation applications, *Disabil. Rehabilitation. Assist. Technol.*, 9 (4) (2013), 344-352, <https://doi.org/10.3109/17483107.2013.805825>.
- [9] Pinto de Oliveira, H. F., An Affordable and Practical 3D Solution for the Aesthetic Evaluation of Breast Cancer Conservative Treatment, (2013). Ph.D. Thesis, Faculdade De Engenharia Da Universidade Do Porto, Programa Doutoral em Engenharia Electrotecnica e de Computadores, Porto.
- [10] Mallick, T., Das, P. P., Majumdar, A. K., Characterizations of noise in kinect depth images: a review, *IEEE Sens. J.*, 14 (6) (2014), 1731-1740, <https://doi.org/10.1109/JSEN.2014.2309987>.